



## Assessing the impact of vegetation cover changes and post-fire effects through an enhanced sediment flow connectivity index (SfCI)

Marina Zingaro<sup>a,\*</sup>, Giovanni Scicchitano<sup>a</sup>, Alberto Refice<sup>b</sup>, Antonella Marsico<sup>a</sup>, Alok Kushabaha<sup>a,c</sup>, Mario Elia<sup>d</sup>, Raffaele Laforteza<sup>d</sup>, Domenico Capolongo<sup>a,b</sup>

<sup>a</sup> Department of Earth and GeoEnvironmental Sciences, University of Bari, via Orabona 4, 70125 Bari, Italy

<sup>b</sup> Institute for the Electromagnetic Sensing of the Environment-Italian National Research Council (IREA-CNR), 70126 Bari, Italy

<sup>c</sup> IUSS – School for Advanced Studies, 27100 Pavia, Italy

<sup>d</sup> Department of Agricultural and Environmental Sciences, University of Bari, Via Amendola 165/A, 70126 Bari, Italy

### ARTICLE INFO

#### Keywords:

Sediment connectivity  
NDVI  
Vegetation cover  
Fires  
Geomorphometry

### ABSTRACT

Land cover plays a fundamental role in surface dynamics that involve sediment connectivity. Land cover types can physically mitigate, prevent or increase sediment production and mobility on the surface. Further, changes in land cover, particularly in vegetation classes, can directly affect these processes, especially if they occur over short time periods or even more rapidly after extreme events such as fires. This study analyses vegetation cover changes in the Lama Camaggi catchment (southern Italy) in relation to its sediment connectivity pattern, described by Sediment flow Connectivity Index (SfCI). The Normalized difference vegetation index (NDVI), derived from satellite data, is utilized to detect vegetation cover changes over 8-year interval and following fire events. The main objective is to evaluate how the NDVI improves the flexibility of SfCI in defining surface dynamics on both spatial and temporal scales. The findings indicate that (1) NDVI changes identify vegetation cover changes in a short period in many areas of the catchment, potentially affecting sediment connectivity, and (2) the implementation of NDVI in the SfCI helps detect post-fire effects on sediment mobility and connectivity. Integrating NDVI enhances the SfCI algorithm providing a more dynamic description of sediment patterns.

### 1. Introduction

Sediment connectivity is a key geomorphological indicator to define sediment pathways in a catchment (Baartman et al., 2013; Bracken et al., 2015; Brierley et al., 2006; Faulkner, 2008; Hooke, 2003; Poepl et al., 2017; Wohl, 2017). The quantitative evaluation of the spatial relationship between components of the landscape system (structural connectivity) and of the relative connection dynamics (functional connectivity) helps to monitor the geomorphological evolution of the Earth surface (Fryirs, 2013; Heckmann and Schwanghart, 2013; Turnbull et al., 2008; Wainwright et al., 2011). Sediment connectivity indices and models contribute to estimate the processes of erosion, transport and deposition by considering various factors affecting material detachment and transfer in a catchment (Ali et al., 2018; Baartman et al., 2020; Borselli et al., 2008; Cavalli et al., 2016; Grauso et al., 2018; Heckmann et al., 2018; Najafi et al., 2021; Zingaro, 2021). Land cover is one of

these factors (Oliveira et al., 2024). Indeed, land cover types can physically mitigate, prevent or increase sediment production and mobility due to the influence on runoff and water erosion (Dunjó et al., 2004; García-Ruiz, 2010; Hooke et al., 2017; Ludwig et al., 2007; Sandercock and Hooke, 2011). As demonstrated in the literature, bare or sparsely vegetated soil exhibits greater susceptibility to sediment detachment and mobilization compared to soil covered by dense vegetation or urban areas (Calsamiglia et al., 2018; Cevasco et al., 2014; Fox et al., 2012; Lizaga et al., 2018; Mohammad and Adam, 2010). It follows that land cover data are often required especially to evaluate the impact of surface cover on the degree of connectivity (Borselli et al., 2008; David et al., 2014; Ludwig et al., 2007; Mahoney et al., 2018; Quiñonero-Rubio et al., 2013; Wohl et al., 2017; Zingaro et al., 2019). Further, changes in surface cover, particularly in vegetation classes, can also alter the pattern of sediment connectivity, especially if they occur over a short period of time (Coulthard and Van de Wiel, 2017; González-Romero et al., 2021;

\* Corresponding author.

E-mail addresses: [marina.zingaro@uniba.it](mailto:marina.zingaro@uniba.it) (M. Zingaro), [giovanni.scicchitano@uniba.it](mailto:giovanni.scicchitano@uniba.it) (G. Scicchitano), [alberto.refice@cnr.it](mailto:alberto.refice@cnr.it) (A. Refice), [antonella.marsico@uniba.it](mailto:antonella.marsico@uniba.it) (A. Marsico), [alok.kushabaha@iusspavia.it](mailto:alok.kushabaha@iusspavia.it) (A. Kushabaha), [mario.elia@uniba.it](mailto:mario.elia@uniba.it) (M. Elia), [raffaele.laforteza@uniba.it](mailto:raffaele.laforteza@uniba.it) (R. Laforteza), [domenico.capolongo@uniba.it](mailto:domenico.capolongo@uniba.it) (D. Capolongo).

<https://doi.org/10.1016/j.catena.2024.108474>

Received 18 June 2024; Received in revised form 11 October 2024; Accepted 14 October 2024

Available online 23 October 2024

0341-8162/© 2024 The Authors. Published by Elsevier B.V. This is an open access article under the CC BY-NC-ND license (<http://creativecommons.org/licenses/by-nc-nd/4.0/>).

Guo et al., 2023; Liao and he, 2023; Quiñonero-Rubio et al., 2013). Therefore, to better consider the continuous evolution of surface dynamics that affect and in turn are conditioned by sediment mobility, the connectivity analysis should take into account vegetation cover and its changes.

In this regard, the normalized difference vegetation index (NDVI) is a broadly-used indicator of live green vegetation cover that exploits the characteristic trend of the spectral reflectance curve of vegetation (Curran, 1983; Huang et al., 2021; Jones and Vaughan, 2010). Several studies demonstrated the usefulness of NDVI changes to detect deforested landscapes, urbanized or terraced areas taken away from wild vegetation, crop and soil marks, as well as woodland affected by fires, and bare soils subsequently covered by vegetation (Agapiou et al., 2017; Farrar et al., 1994; Jeevalakshmi et al., 2016; Pettorelli et al., 2005; Sui and Sasser, 2019; Van Leeuwen et al., 2006; Zaitunah et al., 2018; Zhu and Liu, 2015). NDVI is available practically on a global basis with high acquisition frequencies from satellites such as NASA's Landsat mission, or the European Copernicus Sentinel 2 constellation. This makes feasible a frequent update of the components of the connectivity which depend on land cover. In fact, the land cover classes most relevant to the end of determining sediment availability are those connected with the presence/absence of vegetation, which contributes through e.g. its effects on soil erosion, or for the supply of wood and leaf material to the sediment load. Abrupt vegetation cover changes occur especially after hazardous events such as fires, which heavily contribute to the modification of sediment production, availability and displacement.

The Sediment flow Connectivity Index (SfCI) defines sediment pathways through a mapping approach, and it has been demonstrated to be a powerful geomorphic indicator for defining the most sensitive areas to geomorphological modifications in a catchment (Zingaro et al., 2019; Zingaro et al., 2020; Zingaro et al., 2023). The index measures the connection by sediment transport between components of the catchment, taking into account forcing elements (i.e. rainfall), functional aspects (i.e. soil stability and proxy for runoff processes) and structural variables (i.e. topography and land cover) of the sediment connectivity. In particular, the SfCI first considers sediment mobilization within a cell and then assesses the displacement of the mobilized sediment along flow paths, estimating sediment linkages between cells. The sediment mobility is the fundamental component of the index, based on two assumptions: if there is no mobilization, there is no connection, and the greater the mobilization, the higher the likelihood of connection (Zingaro et al., 2019). Land cover is a primary variable in SfCI, serving as one of the key inputs used to generate the sediment mobility map. Specifically, land cover map is considered to derive the land use index, with values determined by the presence and type of vegetation classes. High values are assigned to classes that promote sediment detachment (e.g., poorly vegetated areas, croplands), while low values are assigned to classes that inhibit sediment detachment (e.g., grasslands, pastures, shrubs) (Zingaro et al., 2019; Zingaro et al., 2020; Zingaro et al., 2023). However, although useful, even when updated, land cover map does not always capture rapid vegetation changes, especially those resulting from a fire, which can be a limitation in accurately estimating sediment mobility.

The use of NDVI is therefore effective in detecting vegetation changes, which is valuable for enhancing sediment connectivity analysis over long time scales and in relation to extreme events. Recent studies demonstrated the positive impact of this application (Arabkhedri et al., 2021; Guo et al., 2023; Liao and He, 2023; Liu et al., 2021; Lopez-Vicente et al., 2020; Martini et al., 2020; Vieira et al., 2018), highlighting the need for a comprehensive approach that integrates these methods: the employment of NDVI, the assessment of sediment connectivity, and the analysis of fire effects.

This paper explores the effectiveness of using NDVI to evaluate changes in sediment connectivity in response to rapid changes in vegetation cover, linking the application of the multi-spectral index in sediment connectivity analysis to the use of sediment connectivity in

monitoring the effects of wildfires. The main objective is to assess how NDVI improves the flexibility of the SfCI in describing surface dynamics on both spatial and temporal scales. To achieve this, we (1) estimated NDVI variations in the Lama Camaggi catchment (southern Italy) over an 8-year interval, evaluating potential effects on the sediment connectivity pattern of the catchment, as described in a previous work by Zingaro et al. (2023) through the computation of SfCI, and (2) investigated how NDVI variations following fire events within the same catchment affect connectivity degree, testing the integration of the multi-spectral index into SfCI algorithm. Considering that vegetation cover is the most rapidly varying terrain characteristic among those taken into account for the SfCI computation, integrating NDVI can enhance the flexibility of the connectivity index.

The here proposed approach supports the novel emerging perspective of linking earth observation to land monitoring.

## 2. Materials and methods

### 2.1. Sediment connectivity pattern

Our analysis was carried out over the Lama Camaggi basin (southern Italy) (Fig. 1a) where the sediment connectivity pattern has been identified through SfCI computation, described in a previous work (Zingaro et al., 2023). This study area is interesting for its peculiar geographical, morphological and topographical features (Fig. 1b), as well as for the occurrence of fire events.

Lama Camaggi is a small basin (210 km<sup>2</sup>), characterized by fluvio-karst valley with ephemeral hydrological regime, a moderately variable soil stability and an overall homogeneous gradient of rainfall, land use and topography. In particular, the low spatial variability of these characteristics is evident from: (i) the narrow range of the mean annual precipitation, which falls between 517 and 598 mm/y; (ii) the predominance of cropland (olive groves, fruit and vegetable crops, vineyards) in much of the catchment, while woodlands and wild vegetation are primarily found in the higher southern portion of the catchment; (iii) the generally low slope angles combining with the presence of small hills (Zingaro et al., 2023). The sediment mobility and connectivity patterns identified in the previous study highlighted few hotspots in two key regions of the catchment, where lower soil stability is attributed to the presence of thinner, less permeable soils. In fact, sediment fluxes generally tend to concentrate in these areas of higher mobility, which are located in the southern half of the catchment and a small northern section, where disconnected areas are more widely distributed (Zingaro et al., 2023, Fig. 4). This sediment connectivity pattern is heavily influenced by the climatic, environmental, and topographical characteristics that contribute to a general spatial-temporal stability of surface conditions within the catchment. Rapid changes are primarily triggered by extreme events such as heavy rainfall or fires, and would be thus most noticeable in the surface cover, particularly in the vegetation.

In the SfCI computation, applied to derive the sediment connectivity pattern as detailed in Zingaro et al. (2023), a regional land use map, updated to 2011 (based on locally available data), was utilized as land cover factor to create the Land use Index (LI) map. This LI map, in combination with other variables (Soil Index, Rainfall Index, Slope and Ruggedness), was instrumental in generating the sediment mobility map (Fig. 2). These variables represent dimensionless indices obtained by ranking their values through a qualitative approach based on a priori interpretation of sediment erosion dynamics (Zingaro et al., 2019). Specifically, the highest value of LI (equal to 1) was assigned to the poorly vegetated class, a high value (0.75) to the cropland class, a medium value (0.5) to the woodland class, a low value (0.25) to the grassland, pastures and shrub classes and a null value (0.05) to the urban class. This approach, similarly to the use of C-factor in USLE-RUSLE models (Renard et al., 1997; Wischmeier and Smith, 1978), allows for the differentiation of surface cover based on its capacity to either facilitate or inhibit sediment erosion. LI is considered in the computation

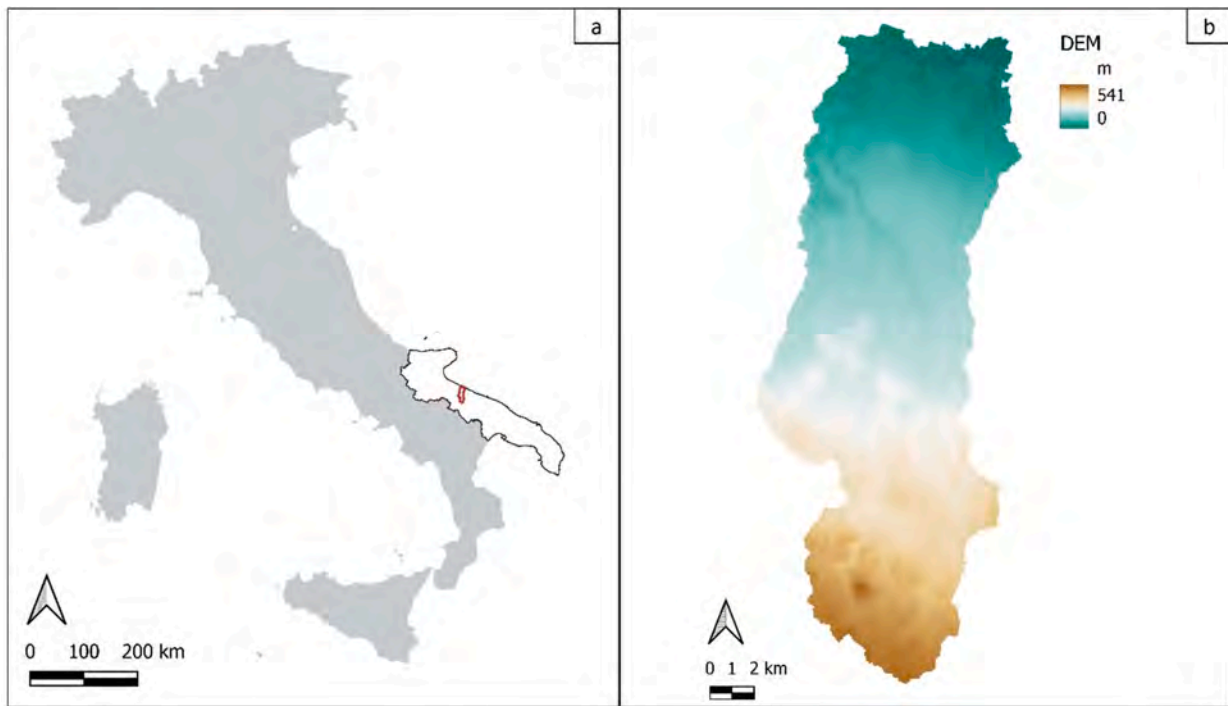


Fig. 1. (a) Lama Camaggi basin location map: the basin (red polygon) is located in the Puglia region (white area) in southern Italy. (b) Elevation map of the basin.

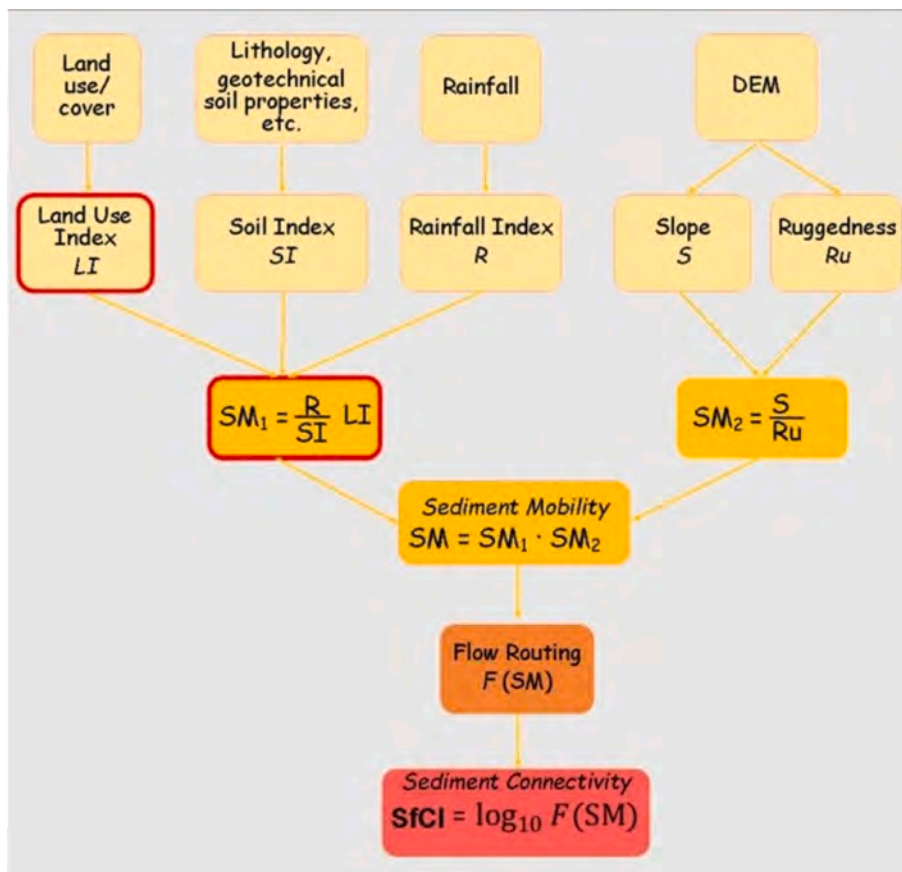


Fig. 2. SfCI algorithm applied in Lama Camaggi catchment. Bordered red rectangles indicate the most rapidly changing variable and the resulting sediment mobility factor (Land use Index-LI and first Sediment Mobility- SM1 respectively).

of a first sediment mobility factor ( $SM_1$ ) which is the base for estimating sediment connectivity together with a second factor ( $SM_2$ ).  $SM_1$  expresses the susceptibility to the sediment detachment,  $SM_2$  expresses the susceptibility to the mobilization of the detached sediment. SfCI is then defined as the outcome of propagating the product of the two preceding factors according to the principle of steepest slope, using the flow accumulation algorithm.

The index maps (input-variables, sediment mobility, SfCI) used for computing sediment connectivity in the Lama Camaggi basin have a spatial resolution of 8 m, determined by the resolution of the digital elevation model (DEM) employed for extracting the morphological features (Zingaro et al., 2023).

## 2.2. NDVI analysis for the detection of vegetation cover changes

The first assessment of this study focuses on the potential to detect changes in vegetation cover within the Lama Camaggi basin during the period following the 2011 update of the land cover map used in the SfCI calculation, utilizing NDVI. This analysis aims to evaluate whether vegetation changes could impact the degree of connectivity, thereby highlighting the need to enhance the SfCI algorithm.

NDVI analysis was applied through satellite image processing in the whole hydrographic catchment (Fig. 1b). NDVI is a vegetation index extracted from multi-spectral images by the ratio between red and near-infrared bands (Jones and Vaughan, 2010). The analysis considered a period of 8 years according to the reference year of the land cover used in SfCI calculation and the availability of satellite images. In particular, the following steps were performed:

1. Selection and download of Sentinel-2 Multispectral Instrument (MSI) data over the study area: one image acquired in the year 2015 was considered, which is the closest to the reference year (2011) based on the availability of the images following satellite deployment. To analyse temporal changes in the vegetation cover, one image acquired in the year 2023 in the same month as the previous (2015) image, was selected. These data were collected through Copernicus Browser (<https://dataspace.copernicus.eu>; accessed on 08/05/2024) and Google Earth Engine platform (<https://earthengine.google.com>; accessed on 08/05/2024).
2. Calculation of NDVI from the selected satellite images through the following equation using the ESA-SNAP toolbox an open-source software developed by European Space Agency (version 9.0.0; <https://step.esa.int/main/download/snap-download/>; accessed on 08/05/2024):

$$NDVI = \frac{(NIR - Red)}{(NIR + Red)} \quad (1)$$

3. Computation of differences between the NDVI maps in the two images:

$$\Delta NDVI = NDVI_{(ii)} - NDVI_{(i)} \quad (2)$$

where  $NDVI_{(i)}$  is the NDVI map for year 2015 and  $NDVI_{(ii)}$  is the NDVI map for year 2023.

4. Quantitative and qualitative assessment of vegetation cover changes across the entire catchment through (a) evaluation of NDVI variation and (b) comparison of NDVI changes with the previously computed LI map,  $SM_1$  map and SfCI map (Zingaro et al., 2023). In particular, an NDVI variation threshold (THR) was established by analyzing the histogram of the NDVI difference map of the study area ( $-0.1 < THR < 0.2$ ). This threshold was used to identify significant NDVI changes for estimating the percentage of NDVI variation in relation to the basin extent and for conducting the comparative analysis. It should be specified that NDVI maps were resampled at the same spatial resolution of the connectivity map (8 m) to apply overlap and comparison. The resampling of the maps and the spatial analysis

were carried out using ArcMap™ and QGIS® software. Specifically, the Resample tool from the Raster Processing toolset and nearest-neighbor technique were employed for the geometric transformation of the maps.

## 2.3. NDVI for the detection of post-fire effects in sediment connectivity

The second assessment of this study focuses on the potential to detect changes in SfCI caused by rapid changes in vegetation cover following fire events within Lama Camaggi basin. To achieve this, we tested the integration of NDVI into SfCI algorithm and calculated it under pre- and post- fire conditions. This analysis aims to evaluate the potential for enhancing the flexibility of SfCI. Changes in sediment mobility and connectivity following fire events in Lama Camaggi basin are identified through the subsequent steps:

1. Selection of fire events for the analysis: a dataset encompassing all fire events in the Puglia region was used to select events in the Lama Camaggi basin. Selection criteria were based on (i) the date of the occurrence within the time interval between the Sentinel-2 satellite acquisitions and (ii) burnt areas larger than 30 ha allowing an analysis at a scale of 8-meter grid resolution. The fire events dataset was derived from the Comando Unità forestali, Ambientali e Agro-alimentari (CUFA, 'Command of the Forest, Environmental and Agro-food units'), Carabinieri Force, and Forestry Services of Autonomous Regions. This data set corresponds to georeferenced polygons recorded between 2000 and 2021 in the Puglia region.
2. Selection and download of Sentinel-2 MSI: for each fire event, one image acquired immediately before and one image acquired immediately after the event were chosen based on image availability.
3. Calculation of NDVI from selected satellite images (pre- and post- for each event) using the method described in the previous paragraph (point 2, paragraph 2.2).
4. Computation of SfCI in the Lama Camaggi catchment under pre- and post- fire conditions by incorporating NDVI into the model algorithm (Fig. 3): the NDVI map was integrated as land cover variable in  $SM_1$  by replacing LI map, and two different equations were tested. Specifically, NDVI measures vegetation cover, which is considered a potential impediment in the detachment and mobilization of the sediment (Zingaro et al., 2019), thereby being inversely proportional to sediment mobility in the first factor of the model. Therefore, the multiplicative (Fig. 3a) and additive (Fig. 3b) inverses of NDVI were tested within the SfCI algorithm, generating implemented SfCI ( $SfCI_{i1}$  and  $SfCI_{i2}$  respectively). This experimental approach to incorporating NDVI into the SfCI is motivated by the multispectral index proven ability to more accurately and in a more up-to-date describe surface coverage, as supported by the literature (Arabhedri et al., 2021; Guo et al., 2023; Liao and He, 2023; Liu et al., 2021). To implement the NDVI map in  $SM_1$ , NDVI values are rescaled from 0.05 (in order to avoid null values) to 1, similar to the rescaling applied to LI and the other variables (Soil Index, Rainfall Index, Slope and Ruggedness; see paragraph 2.1). However, the NDVI values were not categorized into classes to preserve their original meaning and variance.
5. Change detection in pre- and post-event NDVI, mobility and connectivity maps in each area affected by the selected fire event: differences between the maps were computed using the same method described in the previous paragraph (point 3, paragraph 2.2). Specifically, Eq. (2) was applied by using pre (i) and post- (ii) fire maps of NDVI,  $SM_1$ ,  $SfCI_{i1}$  and  $SfCI_{i2}$ .
6. Quantitative analysis of the differences between the maps of NDVI,  $SfCI_{i1}$  and  $SfCI_{i2}$  in the burned area of both fire events. The pixel frequency of each raster was calculated for both positive and negative value classes. This operation is intended to: (1) assess the trend of one raster relative to the other within specific value classes, and (2) identify any differences between  $SfCI_{i1}$  and  $SfCI_{i2}$ .

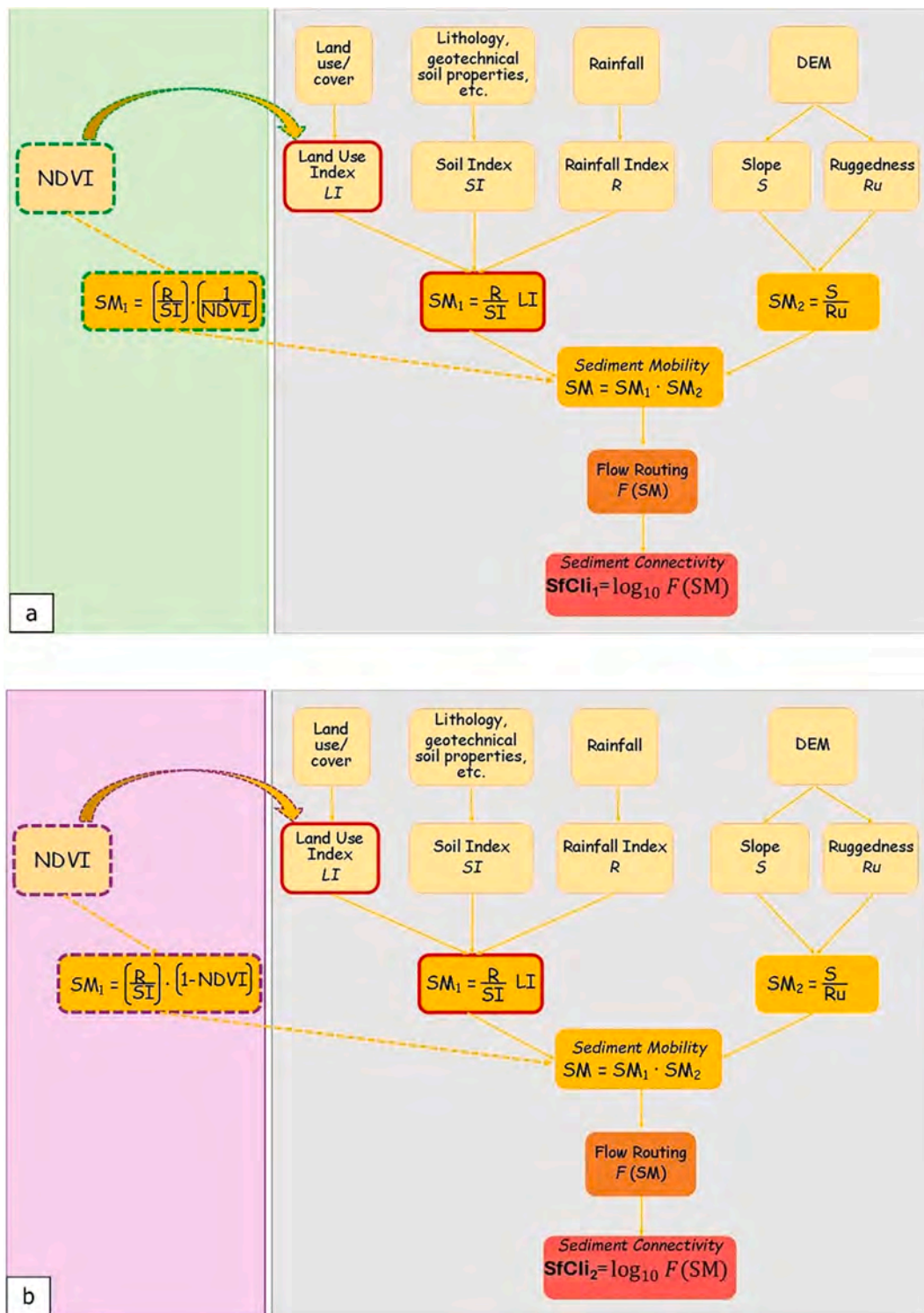


Fig. 3. Implementation of NDVI into the SfCI algorithm through multiplicative (a) and additive (b) inverse equations (green and purple sections, respectively). NDVI (bordered green and purple rectangles, respectively) replaces the land use index in the first sediment mobility factor (bordered red rectangles).

7. Computation of statistics for SfCI (i.e., without NDVI implementation),  $SfCI_1$  and  $SfCI_2$  (in pre- and post- fire dates) maps across the entire Lama Camaggi basin. This analysis aims to observe the variation of the sediment connectivity index over time. In particular, the comparison of the main statistical indicators is intended to evaluate the potential flexibility of the implemented SfCI.

of the statistics were carried out using ArcMap™, QGIS® and MATLAB® software.

### 3. Results

#### 3.1. Vegetation cover changes

Through NDVI analysis, it was possible to evaluate vegetation cover

The computation of the maps, the spatial analysis and the calculation

changes in the study region in the period following the 2011 update of the land cover map used in the SfCI calculation (Zingaro et al., 2023). NDVI was computed from satellite images acquired on 25/05/2015 (selected for the reference year) and 28/07/2023 (selected for the last year). The NDVI differences between maps indicate a rapid and high change in vegetation cover in the catchment. The variation rate of 7.1 % in Lama Camaggi basin (Fig. 4) should be analyzed with respect to the catchment geographical extent (210 km<sup>2</sup>) and the short time frame of detection (8 years).

Fig. 5 shows details of NDVI change map and satellite images for a specific region of Lama Camaggi basin, where NDVI variations are more concentrated. Fig. 6 presents NDVI change, LI, SM<sub>1</sub> and SfCI maps for the same specific region. Areas where significant changes in NDVI occurred were marked in red, allowing the observation of LI, SM<sub>1</sub>, and SfCI values in those same areas. Through this comparison, we were able to assess the quantitative and temporal changes in vegetation cover in the areas where land cover, sediment mobility and sediment connectivity had previously been studied (Zingaro et al., 2023).

Fig. 6 highlights the occurrence of areas (bordered in red) where surface coverage changed as shown already by the visual comparison of Sentinel-2 images (c-d in Fig. 5) and proved by NDVI changes map (b in Fig. 5a in Fig. 6). The latter shows in dark blue areas where NDVI strongly decreases and in yellow areas where NDVI strongly increases, generally identifying bare soils previously covered by vegetation in first case, and the opposite condition in the second case. In particular, most areas in Lama Camaggi basin correspond to LI value (0.75 in b of Fig. 6) indicative of cropland class (see paragraph 2.1 of this work and Table 5 in Zingaro et al., 2023) suggesting that during last years the land may no longer be cultivated (rows of trees or crop plants that can no longer be seen on the surface) or may have been subject to changes of use or cultivation (agricultural structures or greenhouses no longer visible above ground). The visual comparison of NDVI changes with sediment mobility and connectivity maps shows that in Lama Camaggi basin areas with changes in surface coverage are characterized by relatively low mobility and connectivity of sediment (c,d in Fig. 6). This assessment should take into account that the sediment connectivity patterns of study area observed in the maps were described by SfCI (in Zingaro et al., 2023) using land cover not updated at the last year (see paragraphs 2.1, 2.2). Therefore, changes in surface cover may have resulted in changes in surface dynamics and thus in estimated sediment flows, modifying sediment connectivity patterns.

### 3.2. Post-fire effects

Changes in sediment mobility and connectivity following two fire events occurred in Lama Camaggi basin on 29 June 2017 and on 21 June

2021 were detected by incorporating NDVI into the SfCI algorithm. The event that occurred in 2017 affected an area of 213 ha in the southern part of the basin, characterized by the presence of pastures, grassland, shrubs, and some olive groves (Fig. 7a-c). The event that occurred in 2021 affected an area of 44 ha in the central part of the basin, characterized by the presence of shrubs, particularly sclerophyll vegetation (Fig. 7d-f). The two different equations (Fig. 3) were applied using NDVI values computed from selected satellite images acquired on 24/06/2017 and 04/07/2017 (pre- and post-fire, respectively) for the first event, and on 13/06/2021 and 23/06/2021 (pre- and post-fire, respectively) for the second event (Fig. 7).

Fig. 8 presents NDVI, sediment mobility and connectivity variation following the fire event occurred in 2017. The impact is evident in the maps showing changes in NDVI (Fig. 8a), SM<sub>1</sub> (obtained using the first and second inverse equations, represented by the green and purple boxes in Fig. 8b,d, respectively) and SfCI<sub>1-2</sub> (represented by the green and purple boxes in Fig. 8c,e, respectively). Similar to Fig. 5, in the map illustrating NDVI changes, dark blue pixels indicate zones where NDVI decreases significantly (reaching down to -0.57), while yellow pixels denote zones where NDVI does not decrease (the maximum value is 0.2, which suggests stability rather than an increase). These color variations help to identify the post-fire response of vegetation, with dark blue indicating zones generally burned, and yellow representing the opposite condition. The maps of changes in SM<sub>1</sub> and SfCI<sub>1-2</sub> demonstrate that the rise in sediment mobility and connectivity (depicted by orange-red pixels, Fig. 8b-e) coincides with zones of decreased NDVI (Fig. 8a). Conversely, a decrease in mobility (blue pixels, Fig. 8b,d) and connectivity (green pixels, Fig. 8c,e) correspond to zones where NDVI increases. By examining the SM<sub>1</sub> change maps (Fig. 8b,d), the central part is distinguished by minimal fluctuations in sediment mobility (depicted by light yellow pixels), which correspond to a slight decrease in NDVI. It can be observed that SM<sub>1</sub> and SfCI<sub>1-2</sub> maps display very similar variations, with only minor differences in their values. Specifically, the SM<sub>1</sub> change maps obtained from the two different inverse equations have value ranges of -3.98 to 13.08 and -2.09 to 6.33 (green and purple boxes b,d in Fig. 8, respectively). The SfCI<sub>1-2</sub> change maps show value ranges of -4.67 to 4.09 and -4.66 to 4.06 (green and purple boxes c,e in Fig. 8, respectively).

Fig. 9 shows NDVI, sediment mobility and connectivity variation following the fire event occurred in 2021. The maps of changes in NDVI (Fig. 9a), SM<sub>1</sub> and SfCI<sub>1-2</sub> (obtained by using the two different inverse equations, represented by the green and purple boxes in Fig. 9d-e, respectively) confirm the pattern described in Fig. 8: the decrease in NDVI corresponds to an increase in sediment mobility and connectivity, and conversely. Nevertheless, there are zones where NDVI does not decrease (the maximum value is 0.12, which suggests stability rather than an increase). There is a slight difference in the trend between SM<sub>1</sub> and SfCI<sub>1-2</sub> in these areas. Specifically, the values of SM<sub>1</sub> and SfCI<sub>1</sub> appear to increase slightly (green boxes b,c in Fig. 9), while the values of SM<sub>1</sub> and SfCI<sub>2</sub> (purple boxes d,e in Fig. 9) tend to have consistently lower values. Indeed, in Fig. 9, some yellow pixels in a correspond to orange pixels in b-c, blue pixels in d and green pixels in e. Additionally, it is worth noting that the change of SfCI<sub>1-2</sub> ranges (0.04 to 0.29 and 0.07 to 0.8, c,e in Fig. 9, respectively) are: (1) reduced in this burned area compared to the previous one, and (2) contain values around 0, indicating that sediment connectivity (1) has undergone minimal changes, likely due to the smaller extent of the area, and (2) did not increase significantly after this event, likely due to NDVI showing only slight variations as a vegetation response to the fire.

These results, based on a qualitative comparison between the maps, are supported by graphs derived from a quantitative analysis. Fig. 10 presents the results of pixel frequency computation across different value classes for NDVI (cNDVI) and sediment connectivity (cSfCI<sub>1-2</sub>) change raster maps, corresponding to the fire events of 2017 (a-d) and 2021 (e-h). For both fire events, the NDVI change maps (blue bars in the graphs) show a higher frequency of pixels in the value classes below 0,

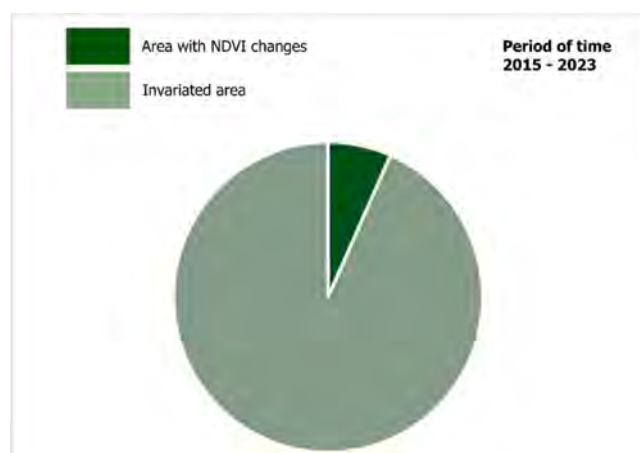


Fig. 4. Graph of NDVI variation during 2015 – 2023 period in the Lama Camaggi basin.

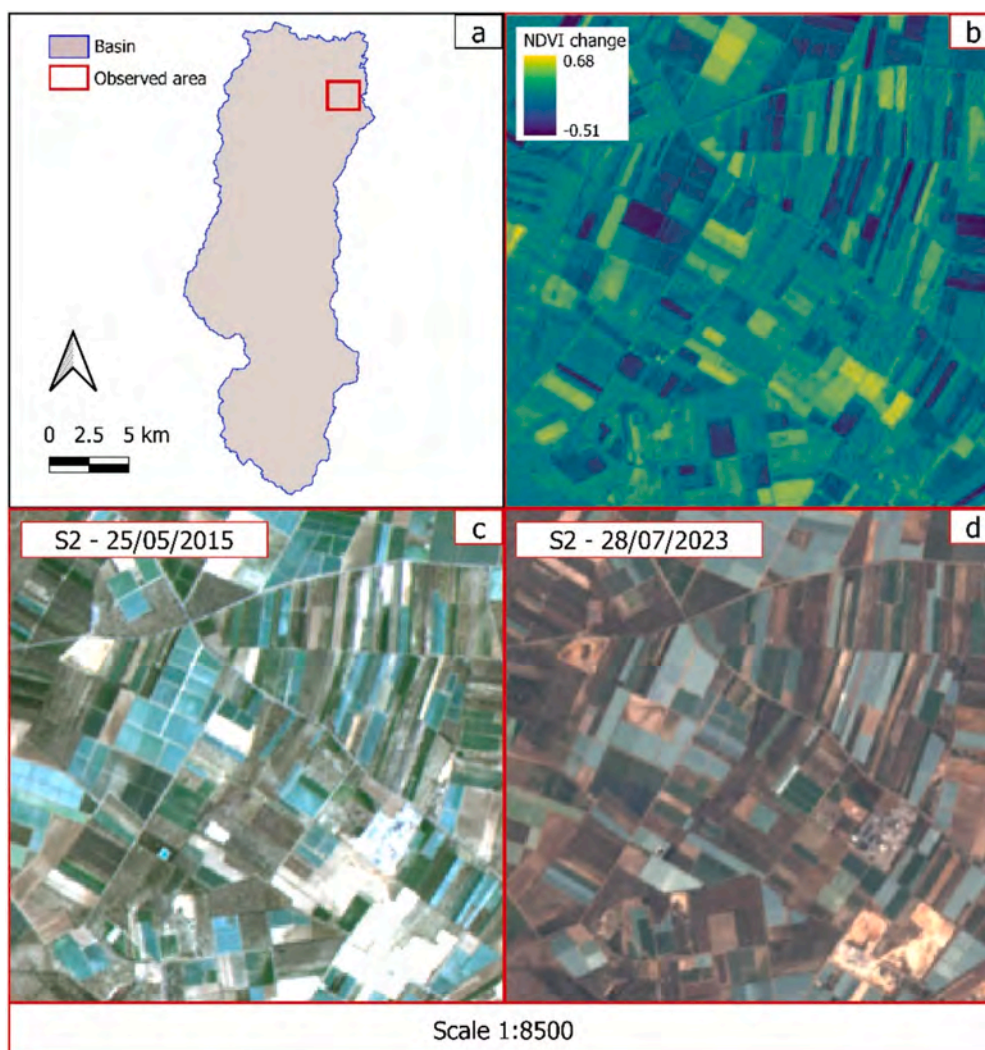


Fig. 5. NDVI analysis in Lama Camaggi basin. (a) Location of the specific region displayed in b-d; (b) NDVI change map; (c,d) Sentinel-2 images.

while the connectivity change maps (light and dark orange bars in the graphs) display a higher frequency of pixels in the value classes above 0. This outcome confirms the trend observed previously, where a decrease of NDVI correspond to an increase of  $cSfCI_{1-2}$ . Furthermore, in 2021 event,  $cSfCI_{1-2}$  maps have no pixels in the negative value classes, as already shown by the Fig. 9e. A difference in pixel frequency between  $SfCI_1$  and  $SfCI_2$  change maps demonstrates a slightly variation on the trend in both fire events. In particular,  $cSfCI_2$  (dark orange bar) displays a greater number of pixels in the higher value class (greater than 0, Fig. 10d,h) compared to  $cSfCI_1$  (light orange bar). This trend seems to be more evident in the event that occurred in 2021, with almost all of the  $cSfCI_2$  pixels falling into the latter class (Fig. 10h), demonstrating a greater susceptibility of this connectivity index ( $SfCI_2$ ) to the decrease in NDVI.

The experimental implementation of NDVI into  $SfCI$  algorithm returned sediment connectivity maps of the lama Camaggi basin, computed in pre- and post- fire dates. Although the overall time interval is quite short (a few years, 2017 to 2021), it is interesting to observe potential differences between  $SfCI_{1-2}$  maps, and compare them with  $SfCI$  map to evaluate the potentially improved flexibility of the index. Table 1 displays the main statistics of  $SfCI$  (classical algorithm, white column) and  $SfCI_{1-2}$  (implemented algorithm, green and purple columns) maps. Almost all statistical indicators show a noticeable change between  $SfCI$  values on the first date (24/06/2017) and  $SfCI$  values on the last date (23/06/2021). In particular, for  $SfCI_1$ , the variations are as

follows: the mean changes by 0.09, the median by 0.1, the first quartile by 0.09, the third quartile by 0.11, the kurtosis by 0.04, and the skewness by  $-0.04$ . For  $SfCI_2$ , the variations are: the mean changes by 0.13, the median by 0.12, the first quartile by 0.13, the third quartile by 0.12, the kurtosis by 0.09, and the skewness by  $-0.03$ .

All the statistics show significant differences between the  $SfCI$  maps (i.e.  $SfCI_{1-2}$  on different dates) and the  $SfCI$  map, proving that the variation in the equation impacts (1) the definition of the sediment connectivity pattern and (2) the dynamism of the index.

#### 4. Discussion

The description of the geomorphological processes that model the surface of a hydrographic basin is based on the analysis of all the factors that play a role in system evolution dynamics. The sediment connectivity indices and models quantitatively define and simulate, respectively, erosion, transport and deposition processes evaluating structural and functional components of the landscape. Land cover is a fundamental property in sediment connectivity assessment for its influence in sediment production and mobility. In fact, the interrelation of surface coverage, runoff and soil erosion influences the sediment connectivity pattern by affecting the availability and the displacement of the sediment (Argentiero et al., 2021; Dunj3 et al., 2004; Sandercock and Hooke, 2011). Therefore, if surface coverage changes, particularly vegetation cover, thus resulting in greater or lesser exposure to runoff and erosion,

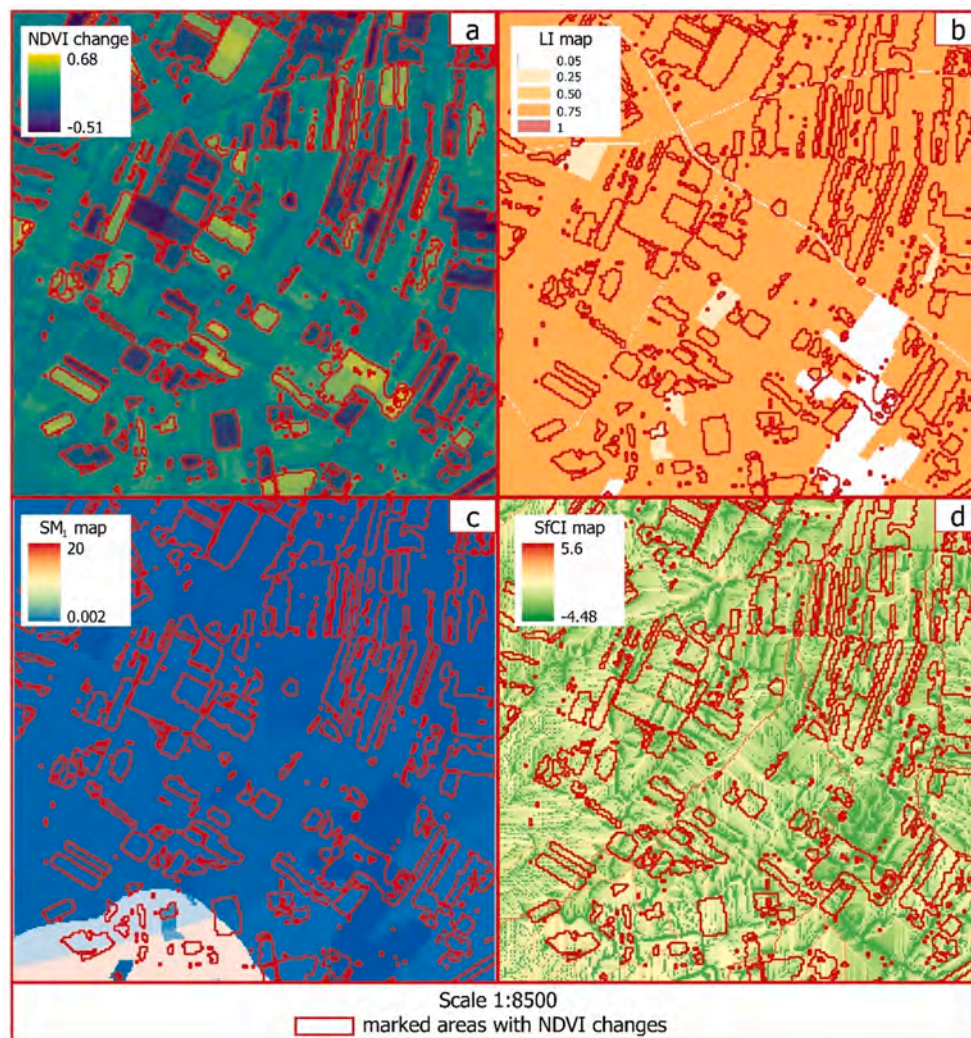


**Fig. 6.** (a-d) Comparison between NDVI change, LI,  $SM_1$  and SfCI map in the specific region located in Fig. 5a. Note: areas marked in red correspond to the areas with significant NDVI changes, tracked also in b-d to observe the values of LI,  $SM_1$  and SfCI computed in the previous study (Zingaro et al., 2023).

sediment dynamics may be altered (Hooke et al., 2017; González-Romero et al., 2021; Coulthard and Van de Wiel, 2017). A connectivity index as SfCI, that is based on the concept of connection by sediment transport, obtained from the propagation of sediment mobility values in flow routing algorithm (Zingaro et al., 2019), should consider this aspect by assessing possible effects of vegetation cover changes on sediment connectivity definition. In particular, vegetation cover changes could influence the first sediment mobility factor ( $SM_1$ ) in which land cover, mainly affected by vegetation presence and type, is a primary variable used to obtain a Land cover Index (LI) map. The possibility of detecting surface coverage changes by NDVI variations over time can contribute to integrate this aspect in SfCI computation. The present study evaluates the use of NDVI to improve the flexibility of SfCI in describing sediment surface dynamics. The experimental application of NDVI in connectivity analysis aims to focus on the factor (vegetation cover) that can change most rapidly than the others (e.g. rainfall, soil stability, topography). To achieve this, two different assessments are applied. The first assessment explores the potential use of this multi-spectral indicator in the Lama Camaggi basin (Fig. 1), where SfCI was previously computed (Zingaro et al., 2023; Fig. 2). This assessment aims to evaluate the potential effects of rapid changes in vegetation cover on sediment connectivity and to determine whether incorporating NDVI could enhance SfCI. The second assessment tests this enhancement by integrating NDVI into the SfCI (Fig. 3) to evaluate how very rapid changes in vegetation cover

following fire events affect sediment connectivity in the Lama Camaggi basin.

The first assessment shows that vegetation cover has changed in a short period with a variable rate, which due probably to the extent of the basin and the time frame detection. Indeed, a variation rate of 7.1 % (Fig. 4) can be considered significant for the small Lama Camaggi catchment over a period of 8 years. It should be noted that changes in surface cover may have occurred in Lama Camaggi catchment during the interval between the year of land cover used in SfCI computation and the year of the first satellite image (2011–2015), which are not detected here due to the unavailability of Sentinel-2 images. However, this aspect would likely extend the period during which vegetation cover changes occurred, without invalidating the detection and analysis of surface coverage variations. The computation of NDVI changes (Fig. 5) and the comparison of them with LI,  $SM_1$  and SfCI maps demonstrates that most vegetation cover changes affect areas belonging to the same land cover class in LI map, i.e. cropland (Fig. 6). This indicates that areas with vegetation cover changes and areas without vegetation cover changes exhibit similar values in LI. Therefore, the potential impact of vegetation cover changes on sediment mobility estimation could be better addressed by implementing NDVI, which exhibits greater variability in its values, into the SfCI algorithm. In fact, the overlap of areas with NDVI variations (marked in red in the Fig. 6) on  $SM_1$  and SfCI maps (c-d in Fig. 6) contributes to evaluate how sediment connectivity pattern could



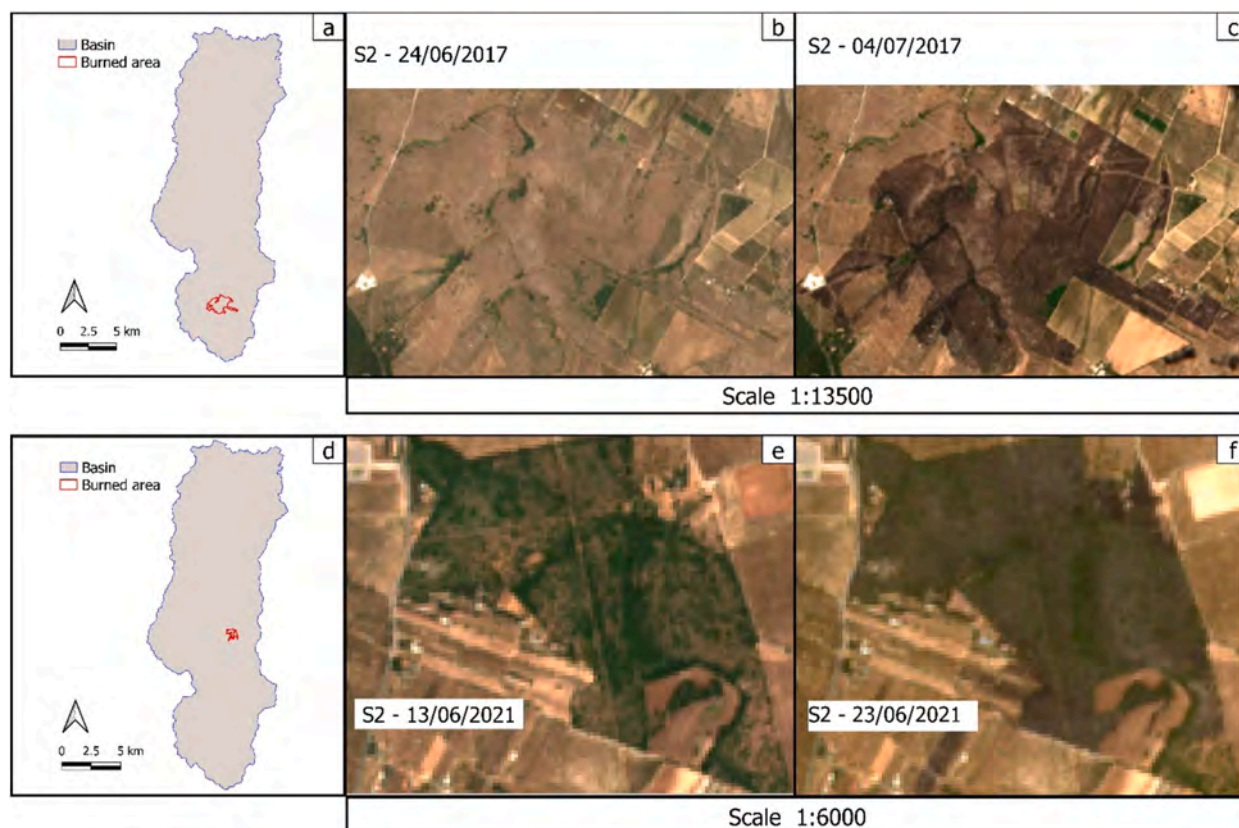


**Fig. 7.** Sentinel-2 images selected for the computation of NDVI in the assessment of post-fire effects in sediment connectivity. (a-c) Location map and S2 images of the area affected by the fire event occurred on 29 June 2017. (d-f) Location map and S2 images of the area affected by the fire event occurred on 21 June 2021.

be influenced by surface cover changes. In particular, areas with changes in NDVI generally correspond to areas characterized by low sediment mobility that could be even lower where NDVI increased, and higher where NDVI decreased, thus reducing or growing connectivity respectively. It should also be noted that in Lama Camaggi catchment the sediment connectivity would be more related to the soil instability (see paragraph 2.1), and thus variations in vegetation cover would play an even more crucial role. Furthermore, given the climatic, environmental and topographical characteristics of the catchment, very rapid changes in vegetation cover can occur following extreme events. Therefore, this assessment shows that the use of NDVI would improve the analysis of sediment connectivity considering the evolution of surface dynamics. The monitoring of vegetation coverage variations could help to better estimate soil erosion and transport in relation to the different exposure of the surface to runoff and sediment production.

The second assessment of the present study tests this feasible improvement by implementing NDVI into the SfCI algorithm ( $SfCI_{1-2}$ ) in order to consider sediment mobility and connectivity changes resulting from very rapid vegetation cover variations following two fire events occurred in the Lama Camaggi basin. The visual comparison of Sentinel-2 images in pre- and post- fire conditions contributes to observe the post-fire effects of the events that affected two large areas of the basin during the summers of 2017 and 2021 years (Fig. 7). Figs. 8 and 9 show the changes in NDVI,  $SM_1$  and the  $SfCI_{1-2}$  following the two events. A prominent pattern seems to emerge: the decrease of NDVI in burned zones aligns with an increase of sediment mobility and connectivity. Conversely, though not uniformly, a lack of change in NDVI in zones less impacted by the fire corresponds to lower values in mobility and connectivity. This trend, confirmed by the pixel frequency graphs (Fig. 10), implies that the response of the vegetation to fire events, which has led to changes in surface cover as described by NDVI, was accurately captured in the calculation of sediment detachment and mobilization,

thereby also affecting the connectivity pattern. Indeed, in the most impacted areas, the fire damages vegetation, leading to soil denudation and exposure, which in turn increases sediment mobility and connectivity. This connection between wildfire severity and sediment connectivity pattern aligns with the findings of López-Vicente et al. (2020) and Martini et al. (2020). The increase of sediment connectivity index, most noticeable in  $SfCI_2$  (see paragraph 3.2 and Fig. 10), indicates that the areas affected by the fire are now more connected with the other parts of the catchment, which receive a greater sediment supply. This result can be considered significant, even when the increase of  $SfCI_{1-2}$  corresponds to values slightly higher than 0, as shown in Figs. 8-10. Indeed, even a small change in the connectivity index can be important from a hydro-graphic catchment management perspective. In fact, given the close connection between sediment connectivity and surface processes, a varied connectivity pattern can affect the dynamics of other surface phenomena, such as landslides and flooding. For example, the high-connectivity pathways described by the index after a fire may indicate increased sediment flow to a channel or down a slope, leading to effects that could trigger extreme events (González-Romero et al., 2021; Zingaro et al., 2019; Zingaro et al., 2020). Therefore, have a constantly updated sediment connectivity index becomes fundamental for a more accurate monitoring of surface dynamics. The statistical analysis of the implemented  $SfCI_{1-2}$  maps demonstrate the variation of the index over time. This analysis shows that a change, albeit small, occurred between 2017 and 2021. Considering the short period and the fact that the area undergoing significant change (due to fire) is small relative to the basin overall extent, this change in the connectivity index can be considered significant. Additionally, it should be noted that in this case, the NDVI implemented in the SfCI was calculated for dates within the same period of the year (June/July). As a result, the NDVI likely varied primarily in the areas affected by the extreme event and less so in others, thereby influencing the range of variation in sediment connectivity index. It can

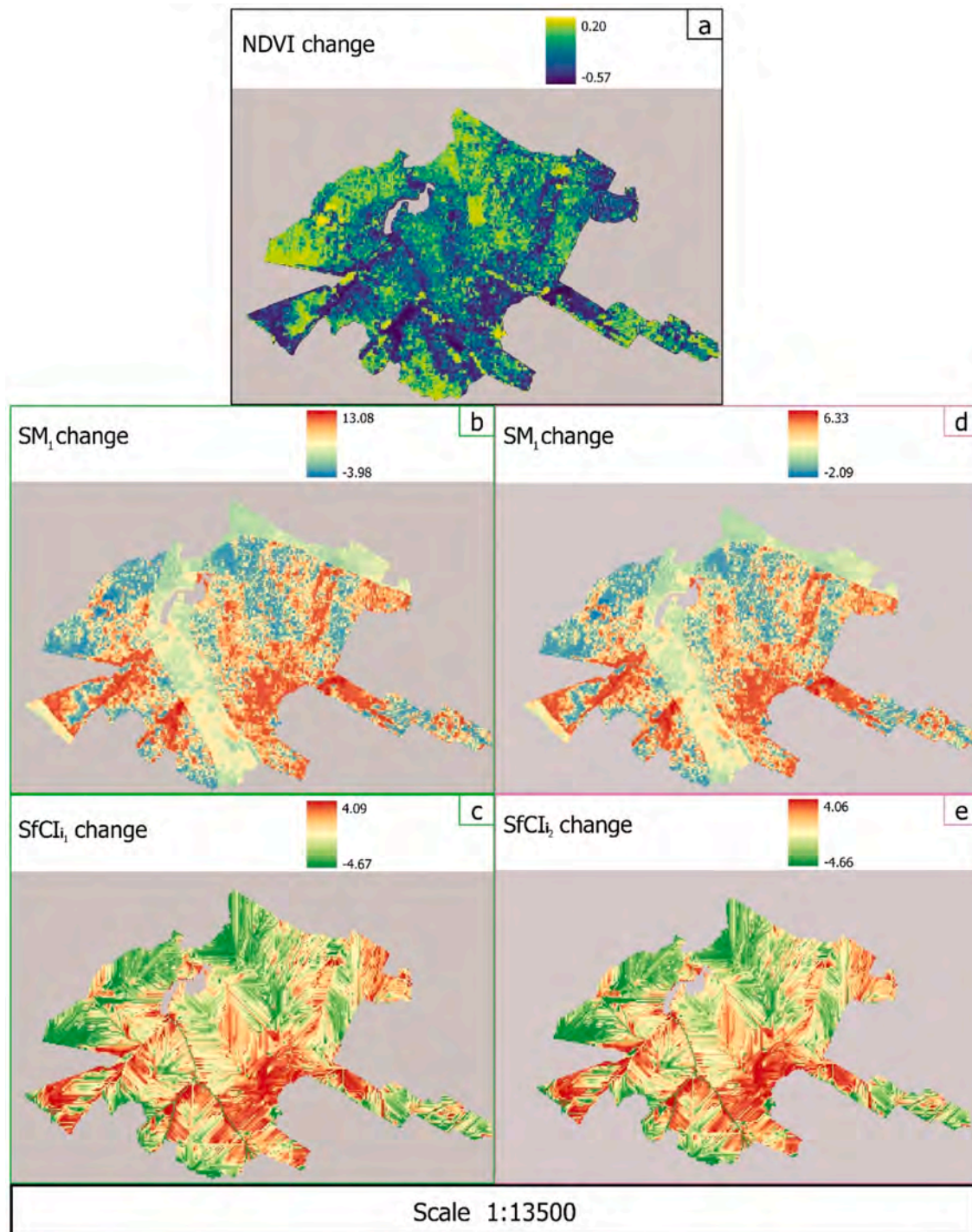


**Fig. 8.** Change detection in the area of the basin affected by the fire event occurred on 29/06/2017. (a-e) Maps of changes in NDVI, sediment mobility ( $SM_1$ ) and connectivity ( $SfCI_{1,2}$ ) of burned area. Note: the green and purple boxes distinguish the maps obtained from the two different inverse equations (see Fig. 3 and text for details).

be inferred that dynamism in the implemented SfCI was achieved, as evidenced by the variations observed in this analysis, which focused on rapid changes in vegetation. Greater dynamism could be observed by considering longer periods, as evidenced by other studies that incorporate NDVI in the computation of the sediment connectivity index, particularly in relation to vegetation cover change (Liao and He, 2023; Liu et al., 2021).

The positive contribution of multi-spectral indices derived from remoted images really lies in an improved description of sediment

patterns on both spatial and temporal scale. Utilizing satellite images makes the connectivity analysis more dynamic by exploiting the possibility to continuously observe surfaces over time and detect changes in very short periods through image processing techniques (Asadi et al., 2023; Zingaro et al., 2022). The integration of satellite remote sensing to account for vegetation cover variations in sediment connectivity represents a new perspective that has the potential to enhance the computation of SfCI and other indices and models. This approach introduces ancillary data and tools that offer essential advantages in

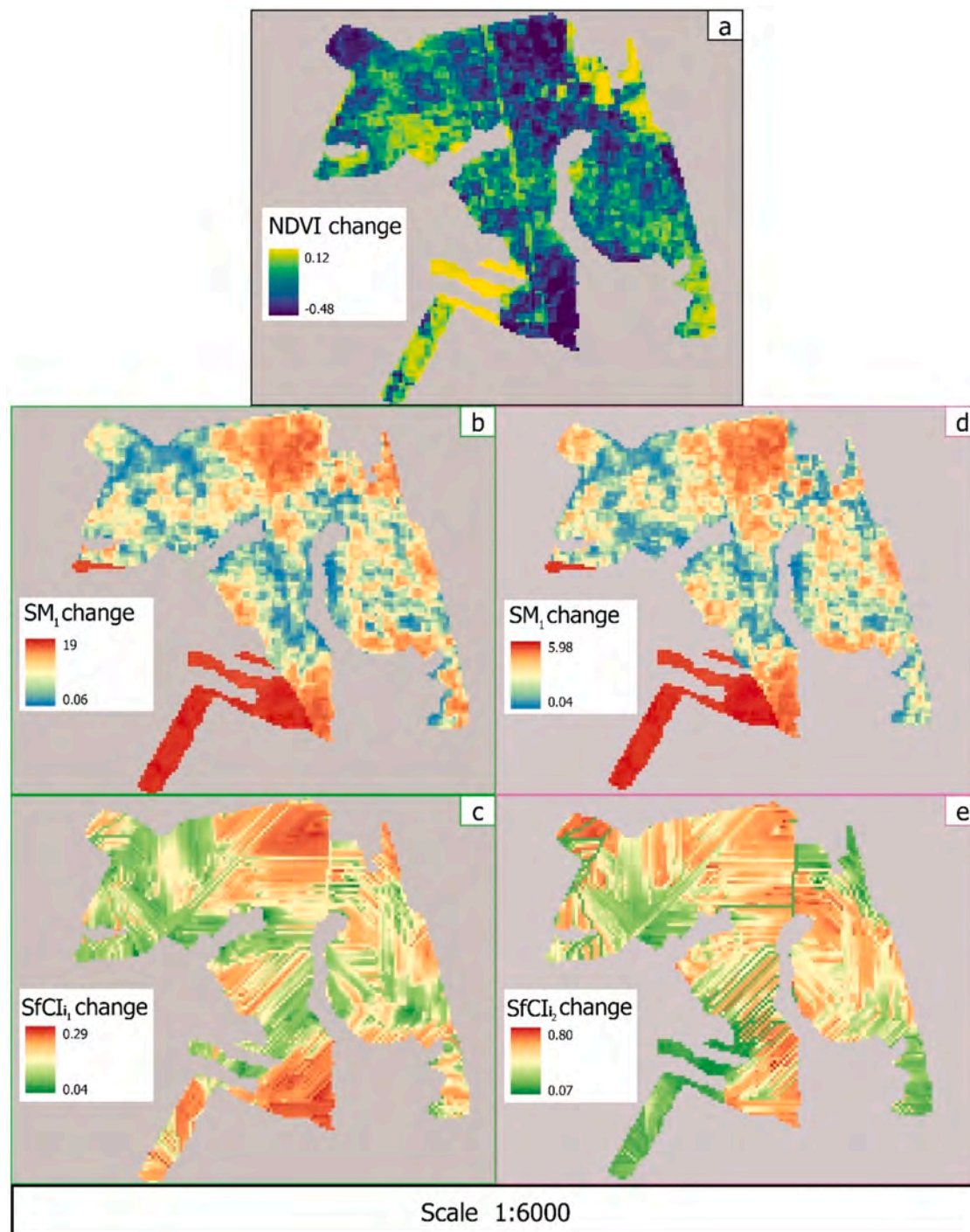


**Fig. 9.** Change detection in the area of the basin affected by the fire event occurred on 21/06/2021. (a-e) Maps of changes in NDVI, sediment mobility ( $SM_1$ ) and connectivity ( $SfCI_{1,2}$ ) of burned area. Note: the green and the purple boxes distinguish the maps obtained from the two different inverse equations (see Fig. 3 and the text for details).

vegetation cover monitoring for the advancement of SfCI.

The latter aspect constitutes the most significant outcome of the present study. However, the work has some limitations, including the limited extent of the burned areas and the lack of ground truth data to demonstrate the effects of rapid vegetation cover changes on sediment yield and delivery in the channels. Further, the results regarding the use of NDVI to estimate the effects of vegetative cover on surface sediment mobility processes may be partially influenced by other factors such as temperature and soil moisture. Therefore, this should be considered a limitation of the study that will need to be addressed and strengthened

in future experiments. Despite these limitations, this study should be viewed as a pioneering effort, offering valuable insights into incorporating vegetation cover changes and post-fire effects into the SfCI algorithm.

## 5. Conclusion

This work explores the use of NDVI to consider rapid vegetation cover changes into SfCI algorithm. The aim was to evaluate the usefulness of NDVI to improve SfCI flexibility. The assessment is conducted in

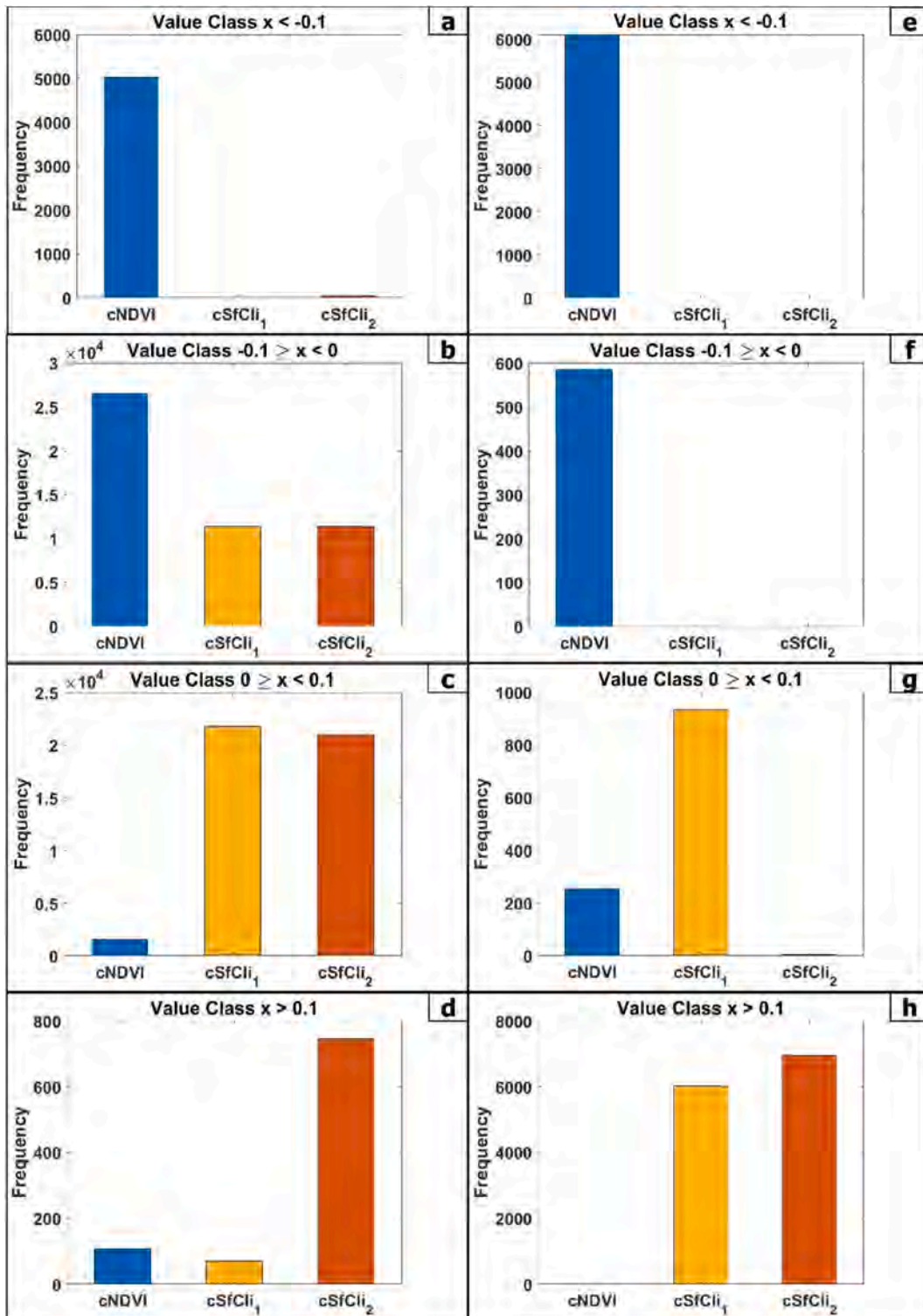


Fig. 10. Bar graphs showing the pixel frequency in value classes of change maps for NDVI (cNDVI, blue bars) and sediment connectivity (cSfCI<sub>1-2</sub>, light and dark orange bars) in the areas affected by the fire events of 2017 (a-d) and 2021 (e-h).

Lama Camaggi basin and includes NDVI calculation and quantitative and qualitative comparative analysis to evaluate the effects of vegetation cover variability on sediment connectivity over short time periods and following fire events. The results can be summarized as follows:

- NDVI detects changes in vegetation cover during a period of 8 years with potential variations of sediment connectivity;
- Rapid changes of vegetation cover following fire events result in increased sediment mobility and connectivity computed by incorporating NDVI into SfCI;
- The varied sediment connectivity pattern is functional for managing the interrelation of surface processes in the catchment;
- The experimental implementation of NDVI in SfCI needs to be further tested in order to improve the algorithm.

**Table 1**

Statistics of SfCI and SfCIi maps over the entire available temporal period in Lama Camaggi basin. Q1 and Q3 are low and upper quartile. Note: the green and purple columns contain the statistics for SfCI<sub>1</sub> and SfCI<sub>2</sub>, respectively.

	SfCI	SfCIi							
	NoTime	24/06/2017		04/07/2017		13/06/2021		23/06/2021	
<b>Maximum</b>	5.65	7.78	7.13	7.70	7.04	7.75	7.01	7.82	7.17
<b>Minimum</b>	-4.48	-4.00	-4.00	-4.00	-4.00	-4.00	-4.00	-4.00	-4.00
<b>Mean</b>	-0.88	1.85	1.19	1.83	1.16	1.82	1.14	1.94	1.32
<b>Standard Deviation</b>	1.57	1.17	1.17	1.17	1.16	1.17	1.16	1.17	1.17
<b>Median</b>	-0.70	1.79	1.14	1.77	1.11	1.76	1.09	1.89	1.26
<b>Q<sub>1</sub></b>	-1.88	1.09	0.42	1.07	0.40	1.06	0.37	1.18	0.55
<b>Q<sub>3</sub></b>	0.19	2.56	1.92	2.54	1.89	2.53	1.87	2.67	2.04
<b>Kurtosis</b>	2.89	6.29	5.49	6.24	5.44	6.26	5.42	6.33	5.58
<b>Skewness</b>	0.03	0.16	0.30	0.15	0.30	0.16	0.30	0.12	0.27

The implementation of multi-spectral indices such as NDVI opens new opportunities for upgrading the SfCI, allowing it to incorporate additional data to describe surface dynamics over time. These improvements would be useful for management decision-making in a hydrographic catchment.

The main advantage of this study is the application of the implemented SfCIi to assess post-fire effects on sediment connectivity, effectively linking the use of NDVI in sediment connectivity assessment with the evaluation of post-fire impacts. However, the main limitation is that the experimentation has only just begun, leaving room for future continuation and refinement in other study areas.

#### CRediT authorship contribution statement

**Marina Zingaro:** Writing – review & editing, Writing – original draft, Visualization, Validation, Supervision, Project administration, Methodology, Investigation, Formal analysis, Data curation, Conceptualization. **Giovanni Scicchitano:** Writing – review & editing, Writing – original draft, Supervision, Methodology, Investigation, Data curation, Conceptualization. **Alberto Refice:** Writing – review & editing, Writing – original draft, Methodology. **Antonella Marsico:** Writing – review & editing, Writing – original draft. **Alok Kushabaha:** Writing – review & editing, Writing – original draft, Investigation. **Mario Elia:** Writing – review & editing, Writing – original draft, Methodology, Investigation. **Raffaele Laforteza:** Writing – original draft. **Domenico Capolongo:** Writing – review & editing, Writing – original draft, Supervision, Methodology, Investigation, Data curation, Conceptualization.

#### Declaration of competing interest

The authors declare that they have no known competing financial interests or personal relationships that could have appeared to influence the work reported in this paper.

#### Acknowledgments

This work is carried out within DEMETRA project, as part of the program “ERC SEEDS UNIBA” by the University of Bari, Italy (Principal Investigator Dr. Marina Zingaro).

#### Data availability

Data will be made available on request.

#### References

- Agapiou, A., Lysandrou, V., Sarris, A., Papadopoulos, N., Hadjimitsis, D., 2017. Fusion of satellite multispectral images based on ground-penetrating radar (GPR) data for the investigation of buried concealed archaeological remains. *Geosciences* 7, 40. <https://doi.org/10.3390/geosciences7020040>.
- Ali, G., Oswald, C., Spence, C., Wellen, C., 2018. The T-TEL method for assessing water, sediment, and chemical connectivity. *Water Resour. Res.* 54, 634–662. <https://doi.org/10.1002/2017WR020707>.
- Arabkhedri, M., Heidary, K., Parsamehr, M.R., 2021. Relationship of sediment yield to connectivity index in small watersheds with similar erosion potentials. *J. Soils Sediments* 21 (7), 2699–2708. <https://doi.org/10.1007/s11368-021-02978-z>.
- Argentiero, I., Ricci, G.F., Elia, M., D'Este, M., Giannico, V., Ronco, F.V., Gentile, F., Sanesi, G., 2021. Combining methods to estimate post-fire soil erosion using remote sensing data. *Forests* 12, 1105. <https://doi.org/10.3390/f12081105>.
- Asadi, H., Dastorani, M.T., Sidle, R.C., 2023. Estimating index of sediment connectivity using a smart data-driven model. *J. Hydrol.* 620, 129467. <https://doi.org/10.1016/j.jhydrol.2023.129467>.
- Baartman, J.E., Masselink, R., Keesstra, S.D., Temme, A.J., 2013. Linking landscape morphological complexity and sediment connectivity. *Earth Surf. Process. Landforms* 38 (12), 1457–1471. <https://doi.org/10.1002/esp.3434>.
- Baartman, J.E.M., Nunes, J.P., Masselink, R., Darboux, F., Biëlders, C., Degré, A., Cantreul, V., Cerdan, O., Grangeon, T., Fiener, P., Wilken, F., Schindewolf, M., Wainwright, J., 2020. What do models tell us about water and sediment connectivity? *Geomorphology* 367, 107300. <https://doi.org/10.1016/j.geomorph.2020.107300>.
- Borselli, L., Cassi, P., Torri, D., 2008. Prolegomena to sediment and flow connectivity in the landscape: A GIS and field numerical assessment. *Catena* 75, 268–277. <https://doi.org/10.1016/j.catena.2008.07.006>.
- Bracken, L.J., Turnbull, L., Wainwright, J., Bogaart, P., 2015. Sediment connectivity: a framework for understanding sediment transfer at multiple scales: Sediment connectivity: sediment transfer at multiple scales. *Earth Surf. Process. Landforms* 40, 177–188. <https://doi.org/10.1002/esp.3635>.
- Brierley, G., Fryirs, K., Jain, V., 2006. Landscape connectivity: the geographic basis of geomorphic applications. *Area* 38, 165–174. <https://doi.org/10.1111/j.1475-4762.2006.00671.x>.
- Calsamiglia, A., Fortesa, J., García-Comendador, J., Lucas-Borja, M.E., Calvo-Cases, A., Estrany, J., 2018. Spatial patterns of sediment connectivity in terraced lands: Anthropogenic controls of catchment sensitivity. *Land Degrad. Dev.* 29, 1198–1210. <https://doi.org/10.1002/ldr.2840>.
- Cavalli, M., Tarolli, P., Dalla Fontana, G., Marchi, L., 2016. Multi-temporal analysis of sediment source areas and sediment connectivity in the Rio Cordon catchment (Dolomites). *Rend. Online Soc. Geol. Ital.* 39, 27–30. <https://doi.org/10.3301/ROL.2016.33>.
- Cevasco, A., Pepe, G., Brandolini, P., 2014. The influences of geological and land use settings on shallow landslides triggered by an intense rainfall event in a coastal

- terraced environment. *Bull. Eng. Geol. Environ.* 73, 859–875. <https://doi.org/10.1007/s10064-013-0544-x>.
- Coulthard, T.J., Van De Wiel, M.J., 2017. Modelling long term basin scale sediment connectivity, driven by spatial land use changes. *Geomorphology* 277, 265–281. <https://doi.org/10.1016/j.geomorph.2016.05.027>.
- Curran, P.J., 1983. Multispectral remote sensing for the estimation of green leaf area index. *Phil. Trans. R. Soc. Lond. A* 309, 257–270. <https://doi.org/10.1098/rsta.1983.0039>.
- David, M., Follain, S., Ciampalini, R., Le Bissonnais, Y., Couturier, A., Walter, C., 2014. Simulation of medium-term soil redistributions for different land use and landscape design scenarios within a vineyard landscape in Mediterranean France. *Geomorphology* 214, 10–21. <https://doi.org/10.1016/j.geomorph.2014.03.016>.
- Dunjó, G., Pardini, G., Gispert, M., 2004. The role of land use–land cover on runoff generation and sediment yield at a microplot scale, in a small Mediterranean catchment. *J. Arid Environ.* 57, 239–256. [https://doi.org/10.1016/S0140-1963\(03\)00097-1](https://doi.org/10.1016/S0140-1963(03)00097-1).
- Farrar, T., Nicholson, S., Lare, A., 1994. The influence of soil type on the relationships between NDVI, rainfall, and soil moisture in semi-arid Botswana. II. NDVI response to soil moisture. *Remote Sens. Environ.* 50, 121–133. [https://doi.org/10.1016/0034-4257\(94\)90039-6](https://doi.org/10.1016/0034-4257(94)90039-6).
- Faulkner, H., 2008. Connectivity as a crucial determinant of badland morphology and evolution. *Geomorphology* 100, 91–103. <https://doi.org/10.1016/j.geomorph.2007.04.039>.
- Fox, D.M., Witz, E., Blanc, V., Soulié, C., Penalver-Navarro, M., Dervieux, A., 2012. A case study of land cover change (1950–2003) and runoff in a Mediterranean catchment. *Appl. Geography* 32, 810–821. <https://doi.org/10.1016/j.apgeog.2011.07.007>.
- Fryirs, K., 2013. (Dis)Connectivity in catchment sediment cascades: a fresh look at the sediment delivery problem: (DIS)Connectivity in catchment sediment cascades. *Earth Surf. Process. Landforms* 38, 30–46. <https://doi.org/10.1002/esp.3242>.
- García-Ruiz, J.M., 2010. The effects of land uses on soil erosion in Spain: a review. *Catena* 81, 1–11. <https://doi.org/10.1016/j.catena.2010.01.001>.
- González-Romero, J., López-Vicente, M., Gómez-Sánchez, E., Peña-Molina, E., Galletero, P., Plaza-Alvarez, P., Moya, D., De Las Heras, J., Lucas-Borja, M.E., 2021. Post-fire management effects on sediment (dis)connectivity in Mediterranean forest ecosystems: Channel and catchment response. *Earth Surf. Processes Landf.* 46, 2710–2727. <https://doi.org/10.1002/esp.5202>.
- Grauso, S., Pasanisi, F., Tebano, C., 2018. Assessment of a simplified connectivity index and specific sediment potential in river basins by means of geomorphometric tools. *Geosciences* 8, 48. <https://doi.org/10.3390/geosciences8020048>.
- Guo, Z., Wu, L., Liu, S., Zhang, H., Du, B., Ruan, B., 2023. An integrated watershed modelling framework to explore the covariation between sediment connectivity and soil erosion. *Eur. J. Soil Sci.* 74 (5), e13412. <https://doi.org/10.1111/ejss.13412>.
- Heckmann, T., Cavalli, M., Cerdan, O., Foerster, S., Javaux, M., Lode, E., Smetanová, A., Vericat, D., Brardinoni, F., 2018. Indices of sediment connectivity: opportunities, challenges and limitations. *Earth-Science Rev.* 187, 77–108. <https://doi.org/10.1016/j.earscirev.2018.08.004>.
- Heckmann, T., Schwanghart, W., 2013. Geomorphic coupling and sediment connectivity in an alpine catchment — Exploring sediment cascades using graph theory. *Geomorphology* 182, 89–103. <https://doi.org/10.1016/j.geomorph.2012.10.033>.
- Hooke, J., 2003. Coarse sediment connectivity in river channel systems: a conceptual framework and methodology. *Geomorphology* 56, 79–94. [https://doi.org/10.1016/S0169-555X\(03\)00047-3](https://doi.org/10.1016/S0169-555X(03)00047-3).
- Hooke, J., Sandercock, P., Cammerata, L.H., Lesschen, J.P., Borselli, L., Torri, D., Meerkerk, A., van Wesemael, B., Marchamalo, M., Barbera, G., Boix-Fayos, C., Castillo, V., Navarro-Cano, J.A., 2017. Mechanisms of Degradation and Identification of Connectivity and Erosion Hotspots. In: *Combating Desertification and Land Degradation*, SpringerBriefs in Environmental Science. Springer International Publishing, Cham, pp. 13–37. [https://doi.org/10.1007/978-3-319-44451-2\\_2](https://doi.org/10.1007/978-3-319-44451-2_2).
- Huang, S., Tang, L., Hupy, J.P., Wang, Y., Shao, G., 2021. A commentary review on the use of normalized difference vegetation index (NDVI) in the era of popular remote sensing. *J. For. Res.* 32, 1–6. <https://doi.org/10.1007/s11676-020-01155-1>.
- Jeevalakshmi, D., Reddy, S.N., Manikiam, B., 2016. Land cover classification based on NDVI using LANDSAT8 time series: A case study Tirupati region. In: 2016 International Conference on Communication and Signal Processing (ICCCSP). Presented at the 2016 International Conference on Communication and Signal Processing (ICCCSP). IEEE, pp. 1332–1335. <https://doi.org/10.1109/ICCCSP.2016.7754369>.
- Jones, H.G., Vaughan, R.A., 2010. *Remote sensing of vegetation: principles, techniques, and applications*. Oxford University Press, Oxford.
- Liao, H., He, Y., 2023. The temporal variation of sediment connectivity from 1982 to 2020 in the Wei River basin, China. *Hydrol. Process.* 37 (12), e15042.
- Liu, W., Shi, C., Ma, Y., Li, H., Ma, X., 2021. Land use and land cover change-induced changes of sediment connectivity and their effects on sediment yield in a catchment on the Loess Plateau in China. *Catena* 207, 105688. <https://doi.org/10.1016/j.catena.2021.105688>.
- Lizaga, I., Quijano, L., Palazón, L., Gaspar, L., Navas, A., 2018. Enhancing connectivity index to assess the effects of land use changes in a mediterranean catchment: effects of land use changes in a mediterranean catchment. *Land Degrad. Develop.* 29, 663–675. <https://doi.org/10.1002/ldr.2676>.
- López-Vicente, M., González-Romero, J., Lucas-Borja, M.E., 2020. Forest fire effects on sediment connectivity in headwater sub-catchments: Evaluation of indices performance. *Sci. Total Environ.* 732, 139206. <https://doi.org/10.1016/j.scitotenv.2020.139206>.
- Ludwig, J.A., Bastin, G.N., Chewings, V.H., Eager, R.W., Liedloff, A.C., 2007. Leakiness: A new index for monitoring the health of arid and semiarid landscapes using remotely sensed vegetation cover and elevation data. *Ecolog. Indic.* 7, 442–454. <https://doi.org/10.1016/j.ecolind.2006.05.001>.
- Mahoney, D.T., Fox, J.F., Al Aamery, N., 2018. Watershed erosion modeling using the probability of sediment connectivity in a gently rolling system. *J. Hydrol.* 561, 862–883. <https://doi.org/10.1016/j.jhydrol.2018.04.034>.
- Martini, L., Faes, L., Picco, L., Iroumé, A., Lingua, E., Garbarino, M., Cavalli, M., 2020. Assessing the effect of fire severity on sediment connectivity in central Chile. *Sci. Total Environ.* 728, 139006. <https://doi.org/10.1016/j.scitotenv.2020.139006>.
- Mohammad, A.G., Adam, M.A., 2010. The impact of vegetative cover type on runoff and soil erosion under different land uses. *Catena* 81, 97–103. <https://doi.org/10.1016/j.catena.2010.01.008>.
- Najafi, S., Dragovich, D., Heckmann, T., Sadeghi, S.H., 2021. Sediment connectivity concepts and approaches. *Catena* 196, 104880. <https://doi.org/10.1016/j.catena.2020.104880>.
- Oliveira, W.L.D., Nero, M.A., Macedo, D.R., 2024. Evaluation of the main variables that influence the sediment connectivity based on applied models. *Geosp.* 28, e-196088. <https://doi.org/10.11606/issn.2179-0892.geosp.2024.196088>.
- Pettorelli, N., Vik, J.O., Mysterud, A., Gaillard, J.-M., Tucker, C.J., Stenseth, N.C., 2005. Using the satellite-derived NDVI to assess ecological responses to environmental change. *Trends Ecology & Evolution* 20, 503–510. <https://doi.org/10.1016/j.tree.2005.05.011>.
- Poeppel, R.E., Keesstra, S.D., Maroulis, J., 2017. A conceptual connectivity framework for understanding geomorphic change in human-impacted fluvial systems. *Geomorphology* 277, 237–250. <https://doi.org/10.1016/j.geomorph.2016.07.033>.
- Quinóner-Rubio, J.M., Boix-Fayos, C., Vente, J.D., 2013. Desarrollo y aplicación de un índice multifactorial de conectividad de sedimentos a escala de cuenca. *Cuadernos de Investigación Geográfica* 39, 203–223. <https://doi.org/10.18172/cig.1988>.
- Renard, K.G., Foster, G.R., Weesies, G.A., McCoole, D.K., Yoder, D.C., 1997. *Predicting Soil Erosion By Water: A Guide to Conservation Planning With the Revised Universal Soil Loss Equation (RUSLE)*. U.S. Department of Agriculture, Agriculture Handbook No. 703.
- Sandercock, P.J., Hooke, J.M., 2011. Vegetation effects on sediment connectivity and processes in an ephemeral channel in SE Spain. *J. Arid. Environ.* 75, 239–254. <https://doi.org/10.1016/j.jaridenv.2010.10.005>.
- Suir, G.M., Sasser, C.E., 2019. Use of NDVI and landscape metrics to assess effects of riverine inputs on wetland productivity and stability. *Wetlands* 39 (4), 815–830. <https://doi.org/10.1007/s13157-019-01132-3>.
- Turnbull, L., Wainwright, J., Brazier, R.E., 2008. A conceptual framework for understanding semi-arid land degradation: ecohydrological interactions across multiple-space and time scales. *Ecohydrology* 1, 23–34. <https://doi.org/10.1002/eco.4>.
- Van Leeuwen, W.J.D., Orr, B.J., Marsh, S.E., Herrmann, S.M., 2006. Multi-sensor NDVI data continuity: Uncertainties and implications for vegetation monitoring applications. *Remote Sens. Environ.* 100, 67–81. <https://doi.org/10.1016/j.rse.2005.10.002>.
- Wainwright, J., Turnbull, L., Ibrahim, T.G., Lertzta-Artza, I., Thornton, S.F., Brazier, R.E., 2011. Linking environmental regimes, space and time: Interpretations of structural and functional connectivity. *Geomorphology* 126, 387–404. <https://doi.org/10.1016/j.geomorph.2010.07.027>.
- Wischmeier, W.H., Smith, D.D., 1978. *Predicting Rainfall Erosion Losses - a Guide to Conservation Planning*. Predicting rainfall erosion losses - a guide to conservation planning, USDA, Science and Education Administration.
- Wohl, E., 2017. Connectivity in rivers. *Prog. Phys. Geography: Earth Environ.* 41, 345–362. <https://doi.org/10.1177/0309133317714972>.
- Zaitunah, A., Samsuri, A., G, A., Safitri, R.A., 2018. Normalized difference vegetation index (ndvi) analysis for land cover types using landsat 8 oli in besitang watershed, Indonesia. In: *IOP conference series: earth and environmental science*, Vol. 126, No. 1. IOP Publishing, p. 012112. <https://doi.org/10.1088/1755-1315/126/1/012112>.
- Zhu, X., Liu, D., 2015. Improving forest aboveground biomass estimation using seasonal Landsat NDVI time-series. *ISPRS Journal of Photogrammetry and Remote Sensing* 102, 222–231. <https://doi.org/10.1016/j.isprsjprs.2014.08.014>.
- Zingaro, M., 2021. Advanced analysis and integration of remote sensing and in situ data for flood monitoring. *Rendiconti Online della Soc. Geol. Ital* 54, 41–47. <https://doi.org/10.3301/ROL.2021.08>.
- Zingaro, M., Refice, A., Giachetta, E., D'Addabbo, A., Lovergine, F., De Pasquale, V., Pepe, G., Brandolini, P., Cevasco, A., Capolongo, D., 2019. Sediment mobility and connectivity in a catchment: a new mapping approach. *Sci. Total Environ.* 672, 763–775. <https://doi.org/10.1016/j.scitotenv.2019.03.461>.
- Zingaro, M., Refice, A., D'Addabbo, A., Hostache, R., Chini, M., Capolongo, D., 2020. Experimental application of sediment flow connectivity index (SFCI) in flood monitoring. *Water* 12, 1857. <https://doi.org/10.3390/w12071857>.
- Zingaro, M., La Salandra, M., Capolongo, D., 2022. New perspectives of earth surface remote detection for hydro-geomorphological monitoring of rivers. *Sustainability* 14 (21), 14093. <https://doi.org/10.3390/su142114093>.
- Zingaro, M., Scicchitano, G., Palmentola, P., Piscitelli, A., Refice, A., Roseto, R., Scardino, G., Capolongo, D., 2023. Contribution of the sediment flow connectivity index (SfCI) in landscape archaeology investigations: test case of a new interdisciplinary approach. *Sustainability* 15, 15042. <https://doi.org/10.3390/su152015042>.